Effects of Precursor Type and Molarity on Phase Stability and Optical Properties of In$_2$O$_3$ Thin Films Deposited by Spray Pyrolysis

- I. Joseph Panneerdoss[*]
- S. Johnson Jeyakumar[**]
- M. Jothibas[**]
- Dr. S. Ramalingam[***]
- M. Bououdina[****]

Abstract

In$_2$O$_3$ thin films were deposited by spray pyrolysis using InCl$_3$ and InNO$_3$ as precursors onto glass substrate. The structural, morphological and optical characteristics have been studied with the variation of precursor concentration. XRD analysis showed the structural orientation of films especially along (222) plane. SEM and AFM studies revealed that the film deposited with 0.10M at 500°C has spherical grains with almost uniform dimension. The band gap energy, refractive index, extinction coefficient and dielectric constants were estimated from U-V absorption data. The variation of these optical parameters with precursor type and its molarity has been investigated. The intense violet light emissions for all the films except the film at 0.15M for InCl$_3$ precursor were observed in the PL spectra. It was observed that resistivity of the films decreased while carrier concentration and mobility increased compared with InNO$_3$ precursor.

Keywords: Precursor; Molarity; SEM; AFM; Transmittance.

Introduction

Highly transparent Indium oxide (In$_2$O$_3$) thin films having wide band gap are very important materials for optoelectronic and gas sensing applications due to their low resistivity and good adherence to substrates [1-3]. Among the various transparent conducting oxides, In$_2$O$_3$ has attracted immense attention due to its enormous applications in many fields, such as optoelectronic devices, thin film solar cells [4] and gas sensors [5].

In$_2$O$_3$ films have been deposited using numerous methods such as reactive evaporation [6], pulsed laser evaporation [7], sputtering [8], sol–gel technique [9], chemical vapour deposition [10] and spray pyrolysis [11] etc. Among these methods, spray pyrolysis technique offers many advantages such as the low cost of the apparatus and source materials, accurate control

[*] Department of Physics, T.B.M.L College, Porayar, Tamil Nadu, India.

[**] Department of Physics, Annamalai University, Annamalai Nagar, Tamil Nadu, India.

[***] Department of Physics, A.V.C College (Autonomous), Mammampandal, Mayiladuthurai, Tamil Nadu, India.

E-mail: ramalingam.physics@gmail.com (Corresponding Author)

[****] Department of Physics, College of Science, University of Bahrain, PO Box 32038, Kingdom of Bahrain.

over the deposition parameters and producing large area films deposition compared to other deposition methods. In_2O_3 films were deposited so far using various precursors, including $InCl_3$, $InNO_3$, In-acetate and In-acac. Among these precursors, $InCl_3$ is a predominant and $InNO_3$ is an infrequent source material for In_2O_3 films deposition.

In the present work, comparative structural, morphological and optical characteristics of sprayed In_2O_3 films deposited from $InCl_3$ and $InNO_3$ as precursors at different molar concentrations was carried out. Initially the characterizations like XRD, SEM with EDAX of deposited films at different temperatures at a constant precursor concentration are studied and the optimum temperature was fixed for both the precursors. Then the optimum molarity was found by various studies of deposited In_2O_3 films for various precursor concentrations with this optimum temperature. The scope of this work is to optimize the molar concentration and precursor of highly transparent conductive In_2O_3 film with optimum properties.

Experimental Details

In_2O_3 films were deposited at different molarities with different precursors ($InCl_3$ and $InNO_3$) by a pneumatic controlled spray pyrolysis. The precursor and deionized water mixture was sprayed onto glass substrate with dimension of 75 x 25 mm^2. During the experiments, the precursor concentration was varied from 0.05M to 0.15M by keeping the substrate temperature and other deposition parameters as constant. In the spray pyrolysis unit, the substrate temperature was maintained with the help of a heater and an electronic circuitry, which contains a thermal sensor with relay switch. The precursor solution and career gas assembly connected to spray gun was moved in the horizontal plane by means of pneumatic controlled system. The substrate to nozzle distance was maintained at 25 cm with an angle of 45°. The films deposited on pre-cleaned glass plates were gradually cooled to room temperature and then rinsed with deionized water and dried.

The well-adherent In_2O_3 films underwent structural, morphological and optical studies. The structural study

was carried out using SHIMADZU-6000 diffractometer equipped with CuKα radiation (λ=1.5418 Å). The surface morphology was examined by HITACHI, S-3400N scanning electron microscope (SEM) equipped with electron dispersive X-ray spectroscopy (EDS) and NANONICS MV 1000 atomic force microscopy (AFM). The optical and photoluminescence spectra were recorded using JASCOV-670 spectrophotometer and Plorolog3-HORIBA JOBIN-YVON, respectively.

Results and Discussion

Structural Studies

The XRD spectra of In_2O_3 films for the molarities 0.05M, 0.1M and 0.15M for the precursor (i) $InCl_3$ and precursor (optimized substrate temperature 500°C) (ii) $InNO_3$ (optimized substrate temperature 400°C) are as shown in Fig. 1. The prominent peaks are in good agreement with the JCPDS Card No-06-0416. Thus the deposited films are polycrystalline in nature with a body centered cubic (bcc) structure having Ia3 space group .The calculated lattice constant for all films is a=10.06Å, which is slightly less than the standard value 10.11 Å [12]. This slight variation of the unit cell dimension is due to tight packing of In_2O_3 cubic crystal.

For $0.05M/InCl_3$, only (222) and (400) reflections are present. But for $0.10M/InCl_3$, the intensity of (400) reflection is reduced and (211), (440) and (622) reflections appear with very low intensity. Only the (222) reflection is present with a very high intensity. For $0.15M/InCl_3$, the intensity of (400) reflection is increased, with (222), (211), (440) and (622) reflections are present with slightly increased intensity.

For $0.05M/InNO_3$, only (222) reflection is present with low intensity. But for 0.10M and 0.15M, (211), (400), (440) and (622) reflections just appear with very low intensity, except (222) reflection is present with a very high intensity.

Among the above prepared films, $InCl_3$ precursor at 0.10M has (222) plane with a very high intensity exhibiting the improved crystalline structure and also degree of film texturing, as I(222)/I(400) ratio, is observed to be maximum.
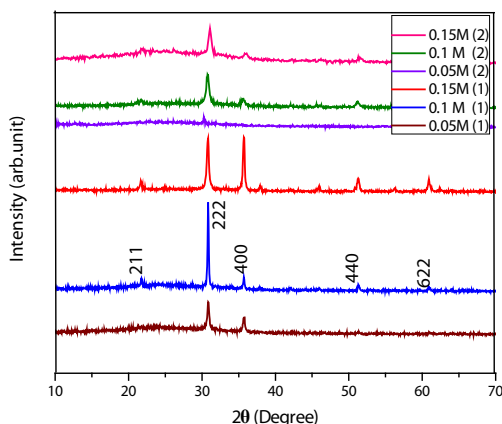
Figure 1: XRD Spectra of In$_2$O$_3$ films at Different Molarities for the Precursors (i) InCl$_3$ and (ii) InNO$_3$

The lattice parameter (a=b=c) was determined using the following equation [16]:

$$d = \frac{a}{\sqrt{h^2 + k^2 + l^2}} \tag{1}$$

where d is the lattice spacing of the crystal planes (h k l)

The crystallite size calculations are carried out from the Scherer-Bragg equation [13]:

$$D = \frac{k\lambda}{\beta \cos\theta} \tag{2}$$

where θ is the Bragg's angle, β is the full width at half maximum of the peaks and λ is the X-ray wave length.

The micro strain (ε) is determined with the relation:

$$\varepsilon = \frac{\beta \cos\theta}{4} \tag{3}$$

The dislocation density (δ) is calculated using the relation:

$$\delta = \frac{1}{D^2} \tag{4}$$

The inter planar spacing (d$_{hkl}$) is calculated using the relation

$$d_{hkl} = \frac{n\lambda}{2\sin\theta} \tag{5}$$

The above structural and micro structural parameters calculated from the (222) reflection, for different precursors/molarities are listed in Table 1. It can be noticed that the 0.10M (1) has the optimized and favorable parameters rather than other molarities, smallest micro strain and dislocations density with an average crystallite size around 18 nm.

Table.1.Grain size, Micro strain, Dislocation density and Inter-planar spacing of In$_2$O$_3$ films at different molarities for the precursors (i) InCl$_3$ and (ii) InNO$_3$

Molar Concentration	Grain size, D (nm)		Micro strain, ε x10^{-3}		Dislocation density, δ x10^{14} (m^{-2})		Inter- planar Spacing (nm)	
	(i)	(ii)	(i)	(ii)	(i)	(ii)	(i)	(ii)
0.05M	26.906	8.676	1.05	4.17	13.813	132.839	0.266	0.140
0.1 M	47.750	18.313	0.76	1.98	4.385	29.817	0.262	0.237
0.15M	27.408	14.486	1.32	2.5	13.311	47.653	0.245	0.431

Surface Morphological Studies

Fig. 2 shows SEM micrographs of In$_2$O$_3$ films with the precursors (i) InCl$_3$ and (ii) InNO$_3$ at three different molarities. For InCl$_3$ precursor, the film at 0.05M shows that the surface is filled by means of very fine grains with some irregularities and 0.10M shows the smoothened film with spherical grains. In the film surface for 0.15M, randomly oriented grains are present due to the higher molarity. For the InNO$_3$ precursor the film at 0.05M showed that the surface filled by means of small grains with some pin holes and for film 0.10M has shown smoothened film with spherical grains. The film surface for 0.15M the randomly oriented grains are present due to the higher molarity. On comparing SEM images of the two precursors, the film at 0.10M having better morphology than the other films for both precursors. Moreover, the film with InCl$_3$ precursor at 0.10M has uncluttered surface morphology. Fig. 3 contains EDS of In$_2$O$_3$ films at 0.1M for InCl$_3$ and InNO$_3$ precursors and it shows that the composition of In and O atomic ratios are 23.5: 76.5 and 14.25: 85.75 respectively.

AFM images of InCl$_3$ and InNO$_3$ precursors at 0.10M as shown in Fig. 4, confirm the results already obtained by SEM analysis. Irregular-shaped particles (close to spherical) in the nanoscale with homogeneous size distribution are observed, forming somehow smooth surface with less porosity.
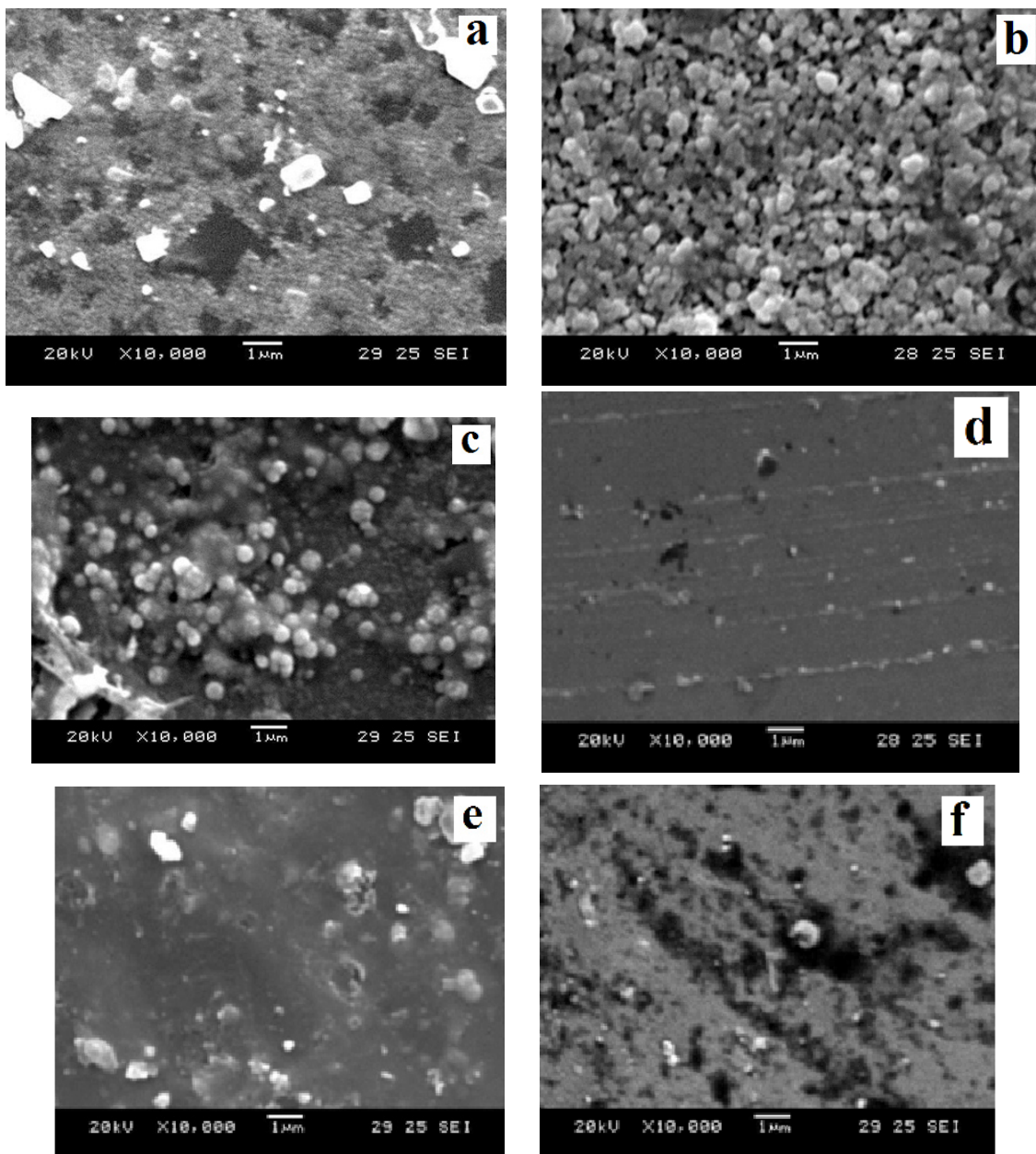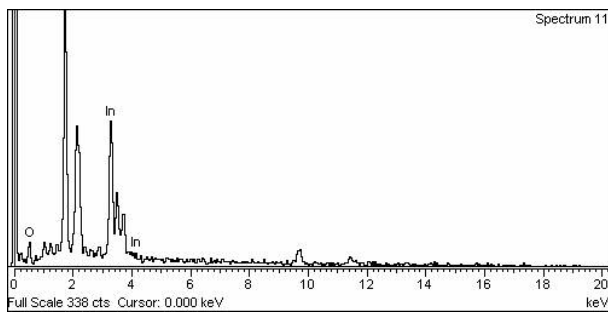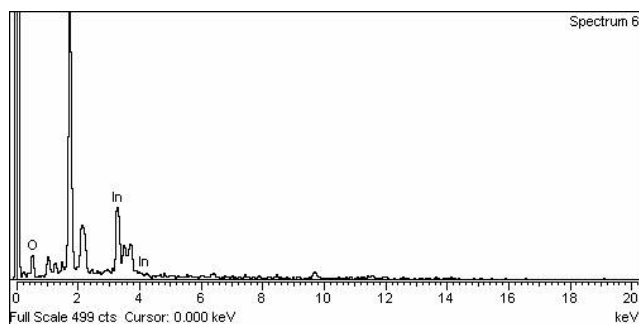
Figure 2: SEM Images of In₂O₃ films at (a) 0.05M (b) 0.1M (c) 0.15M for InCl₃ (d) 0.05M (e) 0.1M (f) 0.15M for InNO₃ Precursors.

(i)

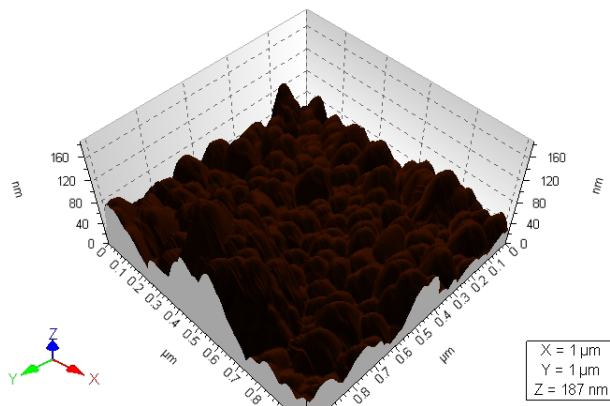**(ii)**

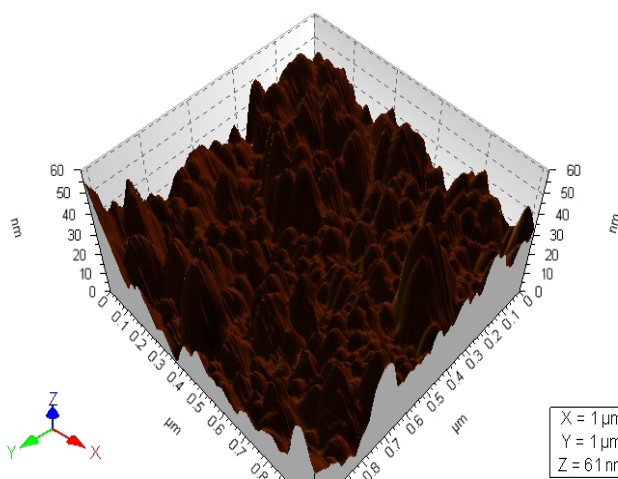**Figure 3: EDS Spectra of In$_2$O$_3$ films at 0.1M for the Precursors (i) InCl$_3$ and (ii) InNO$_3$**

(i)
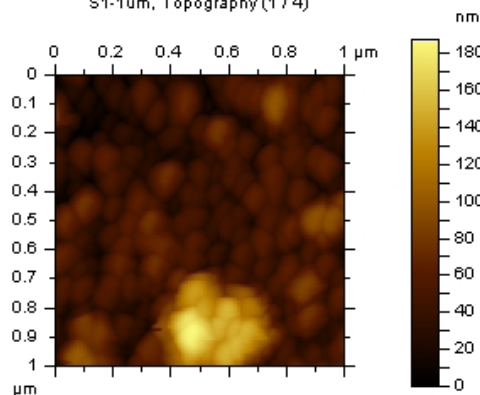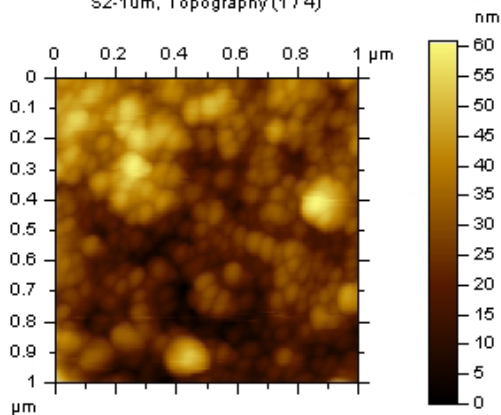
(ii)

Figure 4: 2D and 3D AFM Images of the film for (i) InCl$_3$ (ii) InNO$_3$ Precursors at 0.1M

Optical Properties of In$_2$O$_3$ Films

The optical transmittance spectra of In$_2$O$_3$ films at the molarities 0.05M, 0.1M and 0.15M for the precursors (i) InCl$_3$ and (ii) InNO$_3$ are as shown in fig.5 for the wavelength range of 300 nm to 1200 nm. The percentage of transmittance for all the films is minimum in UV region and maximum in the visible and near infra-red regions. The increasing transmittance percentage is due to uniform oxidation and improved lattice arrangements [14]. From the transmittance spectra, the transmittance percentage for the films at 0.05M and for 0.1M for the InNO$_3$ precursor are maximum and the films at 0.15M for both the precursors are observed to be minimum. The transmittance percentage of the films deposited at 0.05M and 0.1M for InCl$_3$ precursor are nearly maximum and also the film at 0.1M exhibit perfect interference pattern due to well crystallinity as evident from XRD results in fig.1.
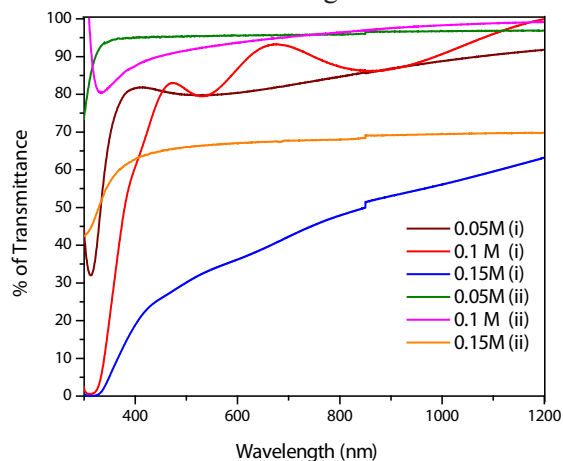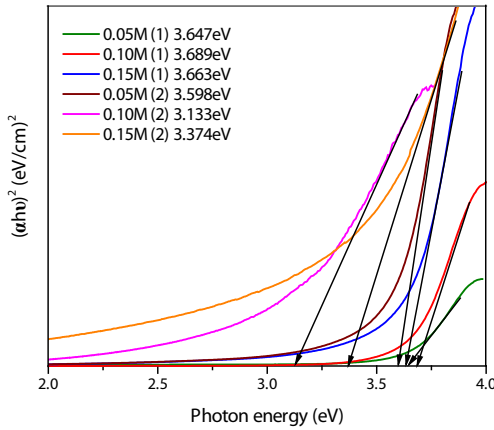

Figure 5: Optical Transmission Spectra of In$_2$O$_3$ Films at Different Molarities for the Precursors (i) InCl$_3$ and (ii) InNO$_3$

The optical band gap of deposited In_2O_3 films is evaluated from the relation between absorption coefficient α and photon energy hν [15].

$$(\alpha h\nu) = A\,(h\nu - E_g)^x \qquad (6)$$

Where A is a constant, E_g is the optical band gap and x =1/2 for directly allowed electronic transitions. The fig.6 shows the plot between $(\alpha h\nu)^2$ and hν of the deposited films at 0.05M,0.1M and 0.15M for the precursors (i) $InCl_3$ and (ii) $InNO_3$.The extrapolation of linear portion of the curves on □ν axis gives the direct band gap energy. The spectra shows that the band gap energy of the films ranging from 3.133 eV to 3.689 eV. The increasing of band gap energy is accredited to the carrier density due to Brustein-Moss effect [16]. The high value of band gap energy for the film at 0.1M for the $InCl_3$ precursor is 3.689eV due to homogeneous and smoothened surface morphology of the film.
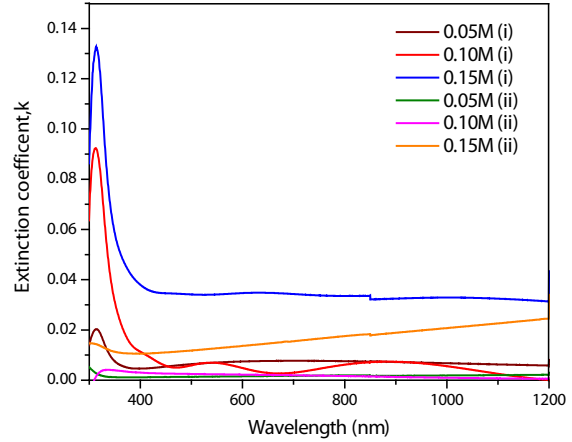

Figure 6: Optical Band Gap Spectra of In_2O_3 Films at Different Molarities for the Precursors (i) $InCl_3$ and (ii) $InNO_3$

The extinction coefficient (k) can be determined using the relation [17]

$$k = \frac{\alpha\lambda}{4\pi} \qquad (7)$$

Fig.7 shows the variation of extinction coefficient with wavelength of In_2O_3 films at different molarities for the precursors (i) $InCl_3$ and (ii) $InNO_3$. In this spectra all the films having maximum k in the U-V region, almost constant and minimum in the visible and near infrared regions. Especially, the spectrum of the film at 0.1M for the $InCl_3$ precursor is revealed better disparity of k between U-V and visible regions than the other molarities and nearly zero extinction coefficient.

The minimum of extinction coefficient or the index of absorption established that the films are highly transparent and without any crystallographic defects. In addition to that, it indicates that the increasing of adhesive nature of the films at 0.1 molarity with the $InCl_3$ precursor.
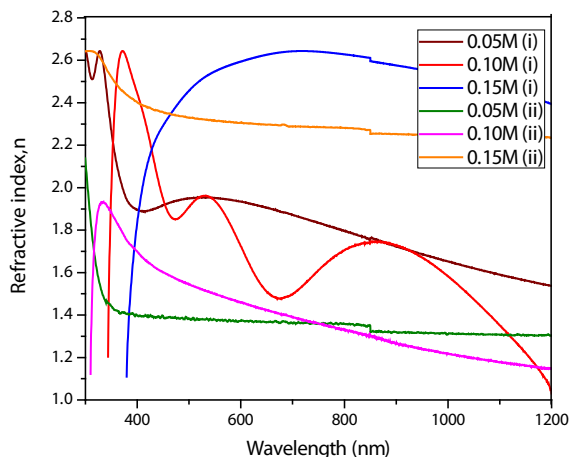

Figure 7: Variation of Extinction Coefficient with Wavelength of In_2O_3 Films at Different Molarities for the Precursors (i) $InCl_3$ and (ii) $InNO_3$

The refractive index (n) of the film can be evaluated using the relation [18]

$$n = \frac{(1+R)^{1/2}}{(1-R)^{1/2}} \qquad (8)$$

Where R is the normal reflectance.Fig.8 shows the variation of refractive index with wavelength of the films at different molarities for the precursors (i) $InCl_3$ and (ii) $InNO_3$. In these spectra for $InCl_3$ precursor, the films deposited for 0.05M and 0.1M having maximum refractive index 2.644 and 2.652 for the wavelengths 327nm and 370nm respectively. The 0.15M exhibits different property as the refractive index is minimum in the U-V region and maximum in the visible and near infrared regions. This may be due to the porosity and pinholes in the film surface with randomly oriented grains. For $InNO_3$ precursor the films deposited at 0.15M having maximum refractive index 2.644 for the wavelength 303nm and 0.05M and 0.1M having maximum refractive index 2.137 and 1.934 for the wavelengths 334nm and 302nm respectively. On comparing the precursors the refractive index is maximum at 0.05M and 0.1M rather 0.15M for $InCl_3$ and for $InNO_3$ is vice-versa.

Figure 8: Variation of Refractive Index with Wavelength of In₂O₃ Films at Different Molarities for the Precursors (i) InCl₃ and (i) InNO₃

The dielectric constant, ε of the films is determined by the relation [19-20]

$$\varepsilon = \varepsilon_1 + \varepsilon_2 = (\varepsilon_1^{\ 2} + \varepsilon_2^{\ 2})^{\ 1/2} \qquad (9)$$

$$\varepsilon_1 = n^2 - k^2 \text{ and } \varepsilon_2 = 2nk \qquad (10)$$

where, ε_1 and ε_2 are the real and imaginary parts of the dielectric constant.

The dielectric constant or the absolute complex permittivity of a material depends on temperature, pressure and frequency, etc. The frequency dependence of real and imaginary parts of the dielectric constant for the films at different molarities for the precursors (i) InCl₃ and (ii) InNO₃ are as shown in fig.9 and fig.10 respectively. From the figures the films at 0.15M for both the precursor exhibit different variation characteristics than the other molarities. The molarities except the film at 0.15M are having maximum value of real and imaginary parts of dielectric constant in the U-V region and minimum in the visible and near infrared regions. Particularly the film at 0.1M for InCl₃ is observed to have the higher values of real and imaginary parts of the dielectric constant than the other molarity deposition, and it may be due electronic, atomic and orientation polarization of the material.
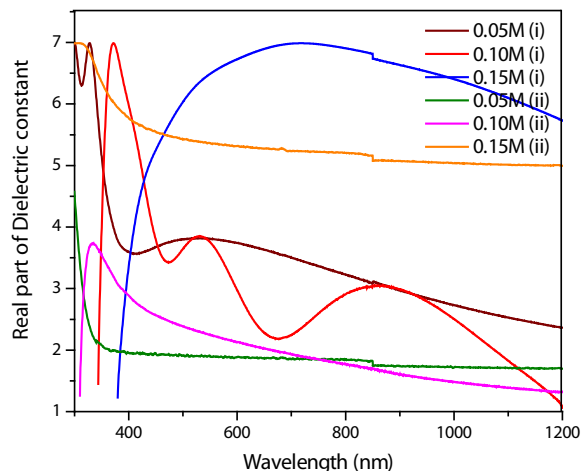
Figure 9: Variation of Real Part of dielectric constant with Wavelength of In₂O₃ Films at Different Molarities for the Precursors (i) InCl₃ and (ii) InNO₃
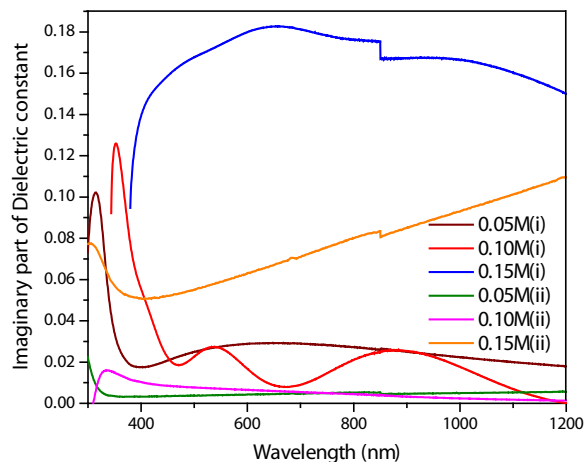
Figure 10: Variation of Imaginary Part of Dielectric Constant with Wavelength of In₂O₃ Films at Different Molarities for the Precursors (i) InCl₃ and (ii) InNO₃

The photoluminescence spectra of In₂O₃ films were obtained using bombardment of an excitation source with wavelength of 325nm.The fig.11 shows the PL spectra of the films deposited at different molarities for the precursors (i) InCl₃ and (ii) InNO₃. In the spectra, for all the films, violet emission is observed except the film at 0.15M for InNO₃ precursor. It emits indigo light with less PL intensity. For the InCl₃ precursor the film at 0.1M alone is having maximum PL intensity. But for the InNO₃ precursor the films at all the molarities are having maximum PL intensity. From photoluminescence spectra of various molarities precursors, the intensity of PL emission and also other optical constants are observed to be maximum for

the film at 0.1M with $InCl_3$ precursor, which implies that more radiative recombination occurs with the excitation source of wavelength of 325nm. The observed optical parameters of In_2O_3 films deposited at different molarities and different precursors are listed in Table.2.

Table 2: Optical Parameters of In_2O_3 Films Deposited at Different Molarities for the Precursors (i) $InCl_3$ and (ii) $InNO_3$

Molarity	Band Gap energy(eV)		Refractive index		Extinction coefficient (minimum value)		Dielectric constant, real part		Dielectric constant, imaginary part		PL intensity x106 (a.u)	
	(i)	(ii)	(i)	(ii)	(i)	(ii)	(i)	(ii)	(i)	(ii)	(i)	(ii)
0 .05M	3.647	3.598	2.644	2.137	0.004	0.001	7.002	4.577	0.101	0.023	2.22	6.59
0.1M	3.689	3.133	2.652	1.934	0.002	0.002	7.015	3.765	0.126	0.016	6.45	6.97
0.15M	3.663	3.374	2.648	2.644	0.034	0.010	6.989	6.989	0.182	0.077	0.20	6.952
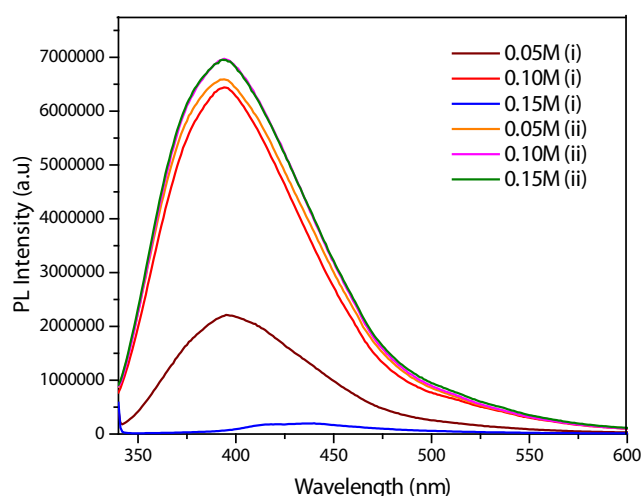
Figure 11: PL Spectra of the Films Deposited at Different Molarities for the Precursors (i) InCl$_3$ and (ii) InNO$_3$

Electrical Properties

The electrical properties are studied for these films prepared at different precursors with optimized molar concentration 0.1M. The hot probe and the Hall Effect measurements have confirmed n-type semiconducting nature of the In_2O_3 films. For the films prepared at $InCl_3$ precursor (0.1M), the carrier density is approximately $3.4 \times 10^{19} cm^{-3}$ with an electrical resistivity of 8.92×10^{-3} Ωcm and mobility 80.2 cm2/Vs have been obtained. Moreover, as the film was prepared with Indium nitrate precursor (0.1M), the carrier density 4.26×10^{18} cm^3 with an electrical resistivity of 1.924×10^{-2} Ωcm and mobility -76.8cm^2/Vs is observed. The resistivity is low for the films prepared at $InCl_3$ that shows the better crystallinity compared with indium nitrate precursor. The Hall Effect result suggested that the In_2O_3 thin films (using InCl3) should be effectively used as optoelectronic application.

Conclusion

In_2O_3 films were deposited by spray pyrolysis using Indium chloride and Indium Nitrate as precursors. The films were deposited at 0.05M, 0.10M and 0.15M. By comparing structural and morphological characteristics, the film deposited at 0.10M for $InCl_3$ precursor has (222) plane as preferred orienting exhibiting improved crystallinity, with maximum grain size and minimum microstrain and dislocation density. The Chlorides are homogeneous anions and Nitrates are heterogeneous anions. So $InCl_3$ is having stronger crystalline structure than $InNO_3$. The optical constants obtained using U-V and PL analysis indicate that the film deposited for 0.10M at 500°C is having band gap energy as 3.689 eV, high refractive index, low extinction coefficient and high intense PL emission. Taking into account that chlorides are more electronegative than nitrates, the nucleation density and deposition rate is higher for the film with $InCl_3$ than $InNO_3$. It could be concluded that structural, morphological and optical characteristics of In_2O_3 films were found to be sensitive to the variation of molarity and precursor, the films with $InCl_3$ as precursor had more advantageous properties than the $InNO_3$. Furthermore, the film deposited at 0.10M with $InCl_3$ shows improved properties, making it suitable for gas sensing and optoelectronic applications.

References

1. Z.M. Jarzebski, Properties of transparent conducting oxide films, Phys. Stat. Sol. (A) 71 (1982)13-41.

2. C.G. Granquist, Electro chromic tungsten oxide films: Review of progress, 1993-1998, Solar energy matter, Solar Cells 60 (2000) 201-262.

3. A.K. Jana, Review of solar cells based on dyes, J. Photochem. Photobiol.A Chem. 132 (2000) 1-17.

4. R.G. Gordon, Criteria for choosing transparent conductors,Mater. Res. Soc. Bull. 25 (2000) 52-57.

5. H. Mexiner, J. Gerblinger, U. Lampe, M. Fleicher, Thin film gas sensors based on semiconducting metal oxides, Sens. Actuators B, B23 (1995) 119-125.

6. E.B. Ali, H.El. Maliki, J.C. Bernede, M. Sahnoun, A. Khelil, O. Saadane, In_2O_3 deposited by reactive evaporation of Indium in Oxygen atmosphere-Influence of post-annealing treatment on optical and electrical properties,Mater. Chem. Phys. 73 (2002) 78-85.

7. D.H. Lowndes, D.B. Geohegan, A.A. Puretzky, D.P. Norton, C.M. Rouleau, Synthesis of novel thin-film materials by pulsed Laser deposition, Science 273 (1996) 898-903.

8. T.L. Barr, Y.L. Liu, An x-ray photo electron spectroscopy study of the valance band structure of Indium oxides, J. Phys. Chem. Solids 50 (1989) 657-664.

9. R.B.H. Tahar, T. Ban, Y. Ohya, Y.Takahashi, Optical, structural and electrical properties of indium oxide thinfilms prepared by the sol-gel method, J. Appl.Phys. 82 (1997) 865-570.

10. J. Kane, H.P. Schweizer, W.Kein, Chemical vapour deposition of transparent electrically conducting layers of Indium Oxide doped with Tin, Thin Solid Films 29 (1975) 155-163.

11. J.C. Manifacier, L. Szepessy, J.F. Bresse, M. Peroten, R.Stuck, In_2O_3:(Sn) and SnO_2:(F) films- Application to solar energy conversion: part 1-preparation and characterization, Mater. Res. Bull. 14 (1979) 109-119.

12. J. Joseph Prince, S. Ramamurthy, B. Subramanian, C. Sanjeeviraja, M. Jayachandran, Spray pyrolysis growth and material properties of In_2O_3 films, Journal of Crystal Growth 240 (2002)142-151.

13. M.Jothibas, C.Manoharan, S.Ramalingam, S.Dhanapandian, S.Johnson Jeyakumar, M. Bououdina, preparation, characterization, spectroscopic (FT-IR, FT-Raman, UV and visible) studies, optical properties and Kubo gap analysis of In_2O_3 thin films, Journal of Molecular Structure 1049 (2013) 239–249.

14. K.L. Chopra, S. Major, D.K. Pandya, Transparent conductors-A status review, Thin Solid Films 102 (1983) 1-46.

15. A.L. Fahrenbruch, R.H. Bube (Eds.), Fundamentals of Solar Cells, Academic, New York, 1993.

16. K.L. Chopra, S.R. Das, Thin Film Solar Cells, Plenum Press, New York,1983.

17. M.Jothibas, C.Manoharan, S.Ramalingam, S.Dhanapandian, M.Bououdina, Spectrochimica Acta Part A: Molecular and Biomolecular Spectroscopy 122 (2014) 171-178.

18. D. Gielo, M.M. Miccocci, R. Rella, P.Siciano and A.Tepore, Optical absorption and photo conductivity in amorphous Indium selenide thin films, Thin Solid Films, 148 (1987) 273-278.

19. F. Yakuphanoglu, S. Ilican, M.Caglar and Y. Caclar, The determination of the optical band and optical constants of non-crystalline and crystalline ZnO thinfilms deposited by spray pyrolysis, J.Optoelect.Adv.Mater., 9 (2007) 2180-2185.

20. M.Jothibas, C.Manoharan, S.Dhanapandian and S.Johnson Jeyakumar, Influence of Precursor Concentration on Sprayed In_2O_3Thin Films, Asian Journal of Chemistry; Vol. 25, Supplementary Issue (2013),S59-S64.